blood® Regular Article

MYELOID NEOPLASIA

Selective targeting of mutated calreticulin by the monoclonal antibody INCA033989 inhibits oncogenic function of MPN

Edimara S. Reis,[1] Rebecca Buonpane,[1] Hamza Celik,[1] Caroline Marty,[2-4] Angela Lei,[1] Fatoumata Jobe,[1] Mark Rupar,[1] Yue Zhang,[1] Darlise DiMatteo,[1] Rahel Awdew,[1] Bianca L. Ferreira,[5] Lynn Leffet,[1] Lu Lu,[1] Elodie Rosa,[2-4] Maxime Evrard,[2-4] Gaurang Trivedi,[1] Brittney Wass,[1] April Horsey,[1] Xin He,[1] Maryanne Covington,[1] Alla Volgina,[1] Florence Pasquier,[2-4,6] Laurence Legros,[7] Guillemette Fouquet,[8] William Vainchenker,[2-4] Yan-ou Yang,[1] Breann Barker,[1] Jing Zhou,[1] Shaun Stewart,[1] Ian S. Hitchcock,[5] Dashyant Dhanak,[1] Ricardo Macarron,[1] Isabelle Plo,[2-4] Horacio Nastri,[1] and Patrick A. Mayes[1]

[1]Incyte Research Institute, Wilmington, DE; [2]INSERM U1287 Gustave Roussy, Université Paris-Saclay, [3]Gustave Roussy, and [4]Université Paris-Saclay, Villejuif, France; [5]Department of Biology, York Biomedical Research Institute, University of York, York, United Kingdom; [6]Hematology Department, Gustave Roussy, Villejuif, France; [7]Clinical Hematology Department, APHP-Hôpital Bicêtre, Le Kremlin-Bicêtre, France; and [8]Clinical Hematology, Centre Hospitalier Sud Francilien, Corbeil-Essonnes, France

KEY POINTS

- **We describe the characterization of INCA033989, a monoclonal antibody that potently and selectively targets mutCALR-positive MPN cells.**
- **Data show the therapeutic potential of INCA033989 as a targeted therapy for MPNs that does not interfere with normal hematopoiesis.**

Mutations in calreticulin (mutCALR) are the second most common drivers of myeloproliferative neoplasms (MPNs) and yet, the current therapeutic landscape lacks a selective agent for mutCALR-expressing MPNs. Here, we show that the monoclonal antibody INCA033989 selectively targets mutCALR-positive cells. INCA033989 antagonized mutCALR-driven signaling and proliferation in engineered cell lines and primary CD34$^+$ cells from patients with MPN. No antibody binding or functional activity was observed in the cells lacking mutCALR. In a mouse model of mutCALR-driven MPN, treatment with an INCA033989 mouse surrogate antibody effectively prevented the development of thrombocytosis and accumulation of megakaryocytes in the bone marrow. INCA033989 reduced the pathogenic self-renewal of mutCALR-positive disease-initiating cells in both primary and secondary transplantations, illustrating its disease-modifying potential. In summary, we describe a novel mutCALR-targeted therapy for MPNs, a monoclonal antibody that selectively inhibits the oncogenic function of MPN cells without interfering with normal hematopoiesis.

Introduction

Myeloproliferative neoplasms (MPNs) are hematopoietic malignancies driven by somatic mutations in multipotent hematopoietic stem cells (HSCs), including polycythemia vera (PV), essential thrombocythemia (ET), and myelofibrosis (MF).[1] Mutations in Janus kinase 2 (*JAK2*), calreticulin (*CALR*), and myeloproliferative leukemia (*MPL*) genes are mutually exclusive and associated with 85% of MPN cases. Although *JAK2* mutations are responsible for disease development in 90% of patients with PV, 60% of patients with ET, and 55% of patients with MF, *CALR* mutations are the second most prevalent and present in 25% and 35% of patients diagnosed with ET and MF, respectively. Mutations in *CALR* are not responsible for PV.[1-3]

Mutations in *CALR* that comprise frameshift insertions or deletions in the *CALR* exon 9 result in the expression of a positively charged C-terminus peptide neoepitope and the loss of the lysine, aspartic acid, glutamic acid, and leucine (KDEL) endoplasmic reticulum (ER)−retention signal that is present in nonmutated wild-type (wt) CALR. A 52-bp deletion (CALR^{del52}) and 5-bp insertion (CALR^{ins5}), also known as type 1 and 2 mutations, respectively, are the most frequent variants among >100 different *CALR* mutations identified so far.[2-4]

The mutant CALR (mutCALR) protein is oncogenic, as it acquires a novel function that involves stable interaction with the thrombopoietin (TPO) receptor (TPOR).[5-8] This interaction originates in the ER and is followed by the transit of the mutCALR/TPOR complex to the cell surface, resulting in a cell surface-exposed neoepitope and constitutive activation of JAK2/signal transducer and activator of the transcription (STAT) signaling downstream of TPOR.[5,8-11]

Patients with mutCALR-driven ET or MF show clonal proliferation of HSCs. Patients with ET develop thrombocytosis and have an increased risk of thrombosis and hemorrhage, whereas patients with MF present with progressive anemia, leukopenia or leukocytosis, thrombocytopenia or thrombocytosis, and extramedullary hematopoiesis. At later stages of the disease, patients may experience debilitating symptoms such as an important splenomegaly, cachexia, bone marrow fibrosis and subsequent hematopoietic failure, leukemic transformation, and premature death.[12-14]

The therapeutic landscape available for patients with MPNs altered dramatically with the approval of the JAK1/2 inhibitor ruxolitinib in 2011 and 2014 for patients with MF and PV, respectively.[15,16] Although current therapeutic options in MPNs provide symptom management and spleen size reduction, they do not impact the underlying mutational allelic burden in most patients and thus are not curative. In addition, some therapies suffer from high rates of discontinuation owing to the emergence of resistance and inadequate drug tolerability. Patients with high-risk ET are usually managed with cytoreductive agents aimed at alleviating symptoms and minimizing thrombosis-related complications, whereas patients with MF are mainly treated with JAK inhibitors.[17-19] Because *CALR* mutations result in a neoepitope expressed on the surface of MPN cells, novel therapeutics that selectively target neoplastic cells expressing mutCALR have the potential to reduce mutCALR allele burden and may allow for eradication of the mutant clone without compromising normal hematopoiesis, consequently improving disease outcomes.[20]

Here, we report the discovery of a monoclonal antibody that selectively targets mutCALR and potently antagonizes its oncogenic function. Our data demonstrate that INCA033989 inhibits abnormal TPOR signaling in MPN cells expressing mutCALR without affecting normal hematopoiesis. These findings highlight the therapeutic potential of INCA033989 as, to our knowledge, the first mutCALR-targeted therapy to enter clinical trials for patients with MPN.

Methods

Surface plasmon resonance (SPR)

Antihuman immunoglobulin G (IgG)–fragment crystallizable (Fc) was coupled to a CM4 chip using an Amine Coupling Kit (Cytiva). INCA033989 was captured on the chip by injecting the designated cells with the sample at a flow rate of 10 μL/min for 30 seconds. The capture levels were in the range of 15 to 25 resonance units. Dilutions of recombinant CALR proteins were injected into cells at a flow rate of 69 μL/min for 150 seconds, followed by a 230-second dissociation phase at the same flow rate. The cell surface was regenerated with a 30-second injection of 3 M $MgCl_2$. Data on the interaction of antibodies with recombinant mutCALR proteins were collected at 25°C using a Biacore 8K instrument (Cytiva). The experiments were conducted using Tris-buffered saline (pH 7.2), 0.005% surfactant P20, and 1 mM $CaCl_2$ as running buffer. Kinetic parameters were obtained by applying a 1:1 binding model to fit the data from multiple-cycle injection experiments using Biacore Insight Evaluation software (version 4.0.8).

Meso Scale Discovery for phospho-STAT5

Ba/F3 and human $CD34^+$ cells were lysed using a cell-signaling lysis buffer with a protease and phosphatase inhibitor cocktail from a pSTAT5a,b Whole Cell Lysate Kit (Meso Scale Discovery). Lysates were then transferred to assay plates and plates were read on a Meso Sector S 600MM plate reader using the Discovery Workbench 4.0 software (Meso Scale Discovery). Inhibition of pSTAT5 signaling was calculated after normalization to maximal (100%) inhibition achieved by cell treatment with 2 to 10 μM of ruxolitinib and no inhibition (0%) in untreated cells.

Cell proliferation

Cell viability was assessed using a CellTiter-Glo Luminescent Cell Viability Assay reagent (Promega) or a CellTiter 96 AQueous One Solution Cell Proliferation Assay (Promega) and a PHERAstar (BMG Labtech), Vi-CELL BLU Cell Viability Analyzer (Beckman Coulter), or a CLARIOstar multimode plate reader (BMG Labtech) for luminescence quantification.

Human primary $CD34^+$ cells and liquid culture

$CD34^+$ hematopoietic stem and progenitor cells (HSPCs) were cultured for 7 days in complete SFEM II media (STEMCELL Technologies) containing penicillin/streptomycin/glutamine (Thermo Fisher Scientific), human stem cell factor (100 ng/mL, Miltenyi Biotec), human Feline McDonough Sarcoma (Fms)-related tyrosin 3 ligand (100 ng/mL; Miltenyi Biotec), TPO (50 ng/mL; Miltenyi Biotec), low-density lipoprotein (10 μg/mL; STEMCELL Technologies), StemRegenin 1 (500 nM; STEMCELL Technologies), UM171 (35 nM; Xcess Biosciences) at 37°C, 5% CO_2. Half-volume of the medium was changed daily for 3 days, followed by a daily complete media change until day 7. Functional experiments were set up if the percentage of $CD34^+$ $Lineage^-$ cells was >70%, as determined by flow cytometry.

Competitive transplantation mouse model

Floxed $CALR^{del52}$ knockin (KI) mice were generated as previously described[21] and were crossed with tamoxifen-inducible Cre-expressing transgenic mice (SCL-Cre-ER^T),[22] resulting in excision of the fused normal exons and expression of the *CALR* gene with the mutated exon 9 after tamoxifen administration (200-mg/kg daily dose; Sigma-Aldrich) for 4 consecutive days.

Lethally irradiated (9.5 Gy) C57BL/6 ($CD45.2^+$) wt recipient mice (Envigo) were engrafted with 3×10^6 cells of a mix of bone marrow cells; 20% from $CD45.2^+$ floxed homozygous $CALR^{del52}$ KI mice and 80% $CD45.2^+$ wt transgenic mice expressing green fluorescent protein (GFP) under the control of the human ubiquitin C promoter (UBI-GFP/BL6).[23] Four weeks after transplantation, KI allele expression was induced by tamoxifen. Two weeks later, 6 mice per group were injected intraperitoneally twice a week with 3 or 10 mg/kg INCA033989 mouse surrogate or isotype for 10 weeks, during which hematologic parameters and chimerism were assessed every 2 weeks. A total of 4 mice were then euthanized for bone marrow and spleen examination, and treatment was halted in another 4 mice that were monitored continuously for an additional 10 weeks to evaluate for relapse. Another 2 mice were euthanized to isolate bone marrow cells for a secondary transplantation into a further 10 lethally irradiated recipient mice. Mouse parameters and chimerism were assessed 4 weeks after transplantation and then

Table 1. Binding of INCA033989 to wt and mutCALR proteins

Analyte	Antibody	k_a ($M^{-1}s^{-1}$)	k_d (s^{-1})	K_D (nM)
MBP-mutCALR^{del52}	INCA033989	1.14×10^6	1.99×10^{-3}	1.75
MBP-mutCALR^{ins5}	INCA033989	8.54×10^5	5.79×10^{-3}	6.78

k_a, association rate constant; k_d, dissociation rate constant; K_D, dissociation constant; MBP, maltose-binding protein.

every 2 weeks for a further 12 weeks (total of 16 weeks) to evaluate for disease onset.

All procedures were approved by the Gustave Roussy Ethic Committee (protocol 2021_032_30958) and Incyte Research Institute (protocols #21-09-089 and #21-11-10). This manuscript describes experiments using blood cells collected from patients with MPN after approved informed consent, following the rules of the internal institutional review boards and the Declaration of Helsinki.

Results

INCA033989 selectively targets mutCALR

INCA033989 was discovered after multiple rounds of selection of single-chain variable fragment phage- and yeast-display libraries with recombinant CALR^{del52} protein as well as peptides derived from the mutCALR C-terminus. INCA033989 was expressed as human IgG1 with an N297A mutation in the Fc region, thus preventing glycosylation in the CH2 domain and silencing the associated Fc-effector functions of the antibody.

We determined the binding kinetics and affinity profile of INCA033989 for recombinant mutCALR proteins using SPR. INCA033989 binds to both recombinant CALR^{del52} and CALR^{ins5} proteins with affinities of 1.75 and 6.78 nM, respectively (Table 1). The slight preferential binding of INCA033989 to CALR^{del52} when compared with CALR^{ins5} is driven by the higher binding association rate constant of INCA033989 to CALR^{del52} when compared with CALR^{ins5} (1.1×10^6 and 8.5×10^5 M^{-1}second^{-1}, respectively) and the lower binding dissociation rate constant of INCA033989 to CALR^{del52} when compared with that of INCA033989 and CALR^{ins5} (1.9×10^{-3} and 5.7×10^{-3} second^{-1}, respectively; Table 1).

INCA033989 selectively targets cells expressing mutCALR and antagonizes mutCALR-induced oncogenic signaling

To investigate the cell binding and functional properties of INCA033989, Ba/F3 and UT-7 cells expressing human TPOR only or human TPOR and mutCALR were generated (Ba/F3-TPOR, Ba/F3-TPOR/CALR^{del52}, UT-7-TPOR, and UT-7-TPOR/CALR^{del52}; supplemental Figures 1 and 2). INCA033989 bound to mutCALR expressed on the surface of Ba/F3-TPOR/CALR^{del52} and UT-7-TPOR/CALR^{del52} cells. Selective targeting of mutCALR was confirmed given the absence of INCA033989 binding to cells expressing TPOR without mutCALR (Figure 1A-B).

Coexpression of TPOR and mutCALR leads to constitutive activation of the JAK/STAT pathway[5,6,8,9] (supplemental Figure 1A). Therefore, the ability of INCA033989 to inhibit mutCALR-induced TPOR signaling was investigated in Ba/F3-TPOR/CALR^{del52} cells using a multiplex fluorescent cell barcoding method (supplemental Figure 3). Treatment with INCA033989 resulted in dose-dependent inhibition of pSTAT3, pSTAT5, phosphorylated extracellular signal-regulated kinase (pERK), phosphorylated mitogen-activated protein kinase kinase (pMEK), phosphorylated protein kinase B (pAKT), and phosphorilated mammalian target of rapamycin (pmTOR) (Figure 1C), indicating that INCA033989 induces broad inhibition of pathogenic TPOR signaling in cells expressing mutCALR. Notably, the fragment antigen–binding region of INCA033989 also showed the ability to inhibit activation of STAT5 (supplemental Figure 2C), confirming that INCA033989 antagonistic properties are not a consequence of receptor crosslinking, that is, the antagonist nature of INCA033989 does not rely on the interaction of the antibody Fc with Fc-receptor in neighboring cells.[24]

In addition to antagonizing mutCALR-induced TPOR signaling, INCA033989 induced a dose-dependent inhibition of cytokine-independent cell proliferation in both Ba/F3 and UT-7 cell lines expressing mutCALR, with a half-maximal inhibitory concentration and 90% inhibitory concentration of 0.1 and 1 μg/mL, respectively (Figure 1D-E).

Furthermore, INCA033989 selectively induced the death of Ba/F3-TPOR cells harboring CALR^{del52} but not JAK2^{V617F}, another MPN driver mutant protein (Figure 1F; supplemental Figure 4), indicating that cytokine-independent proliferation and survival of cells with mutCALR was selectively inhibited by INCA033989.

INCA033989 antagonizes oncogenic function of mutCALR-expressing Ba/F3 cells in vivo

To determine the antagonist function of INCA033989 in an in vivo system, NOD scid gamma (NSG) mice were inoculated IV with Ba/F3-TPOR/CALR^{del52} cells and then treated with a single dose of 10 mg/kg of INCA033989 or isotype control on day 10 after cell inoculation (Figure 2A). Ba/F3-TPOR/CALR^{del52} cells proliferated in vivo and were detected in the blood of mice on day 13 after cell inoculation (Figure 2B). Treatment with INCA033989, but not the isotype control, resulted in decreased numbers of Ba/F3 cells in the blood and spleen, as reflected by a decrease in spleen weight (Figure 2B-C). The plasma concentration of INCA033989 on day 13 was determined to be 50 μg/mL, indicating drug exposure above 90% inhibitory concentration, as determined in the in vitro functional assays above.

To characterize the pharmacokinetics (PK) profile of INCA033989, human neonatal fragment crystallizable receptor (hFcRn) transgenic (hFcRn Tg32) mice were dosed IV with 5 mg/kg of INCA033989, and the plasma antibody concentration was

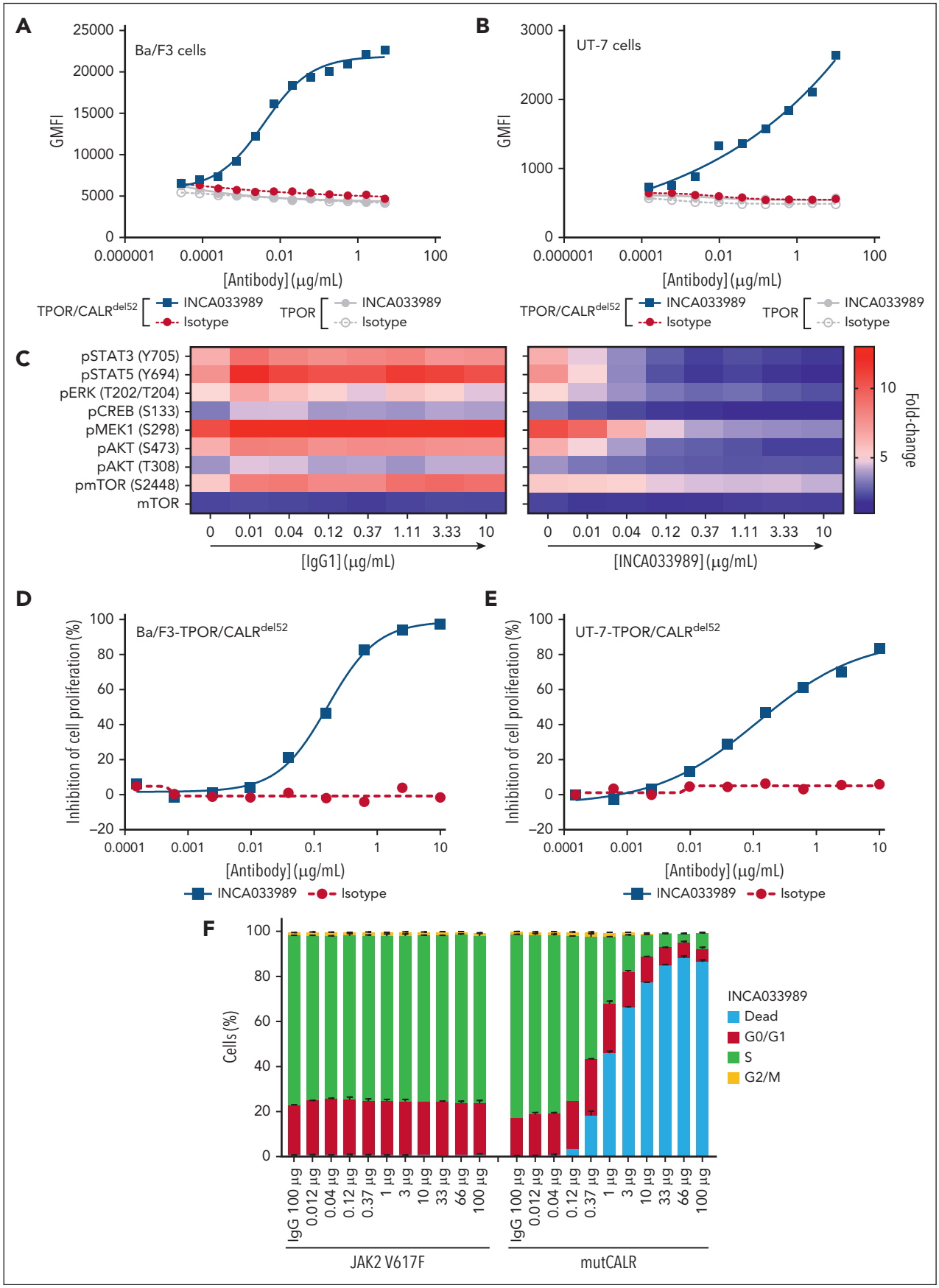
A
Ba/F3 cells
GMFI
[Antibody] (μg/mL)
TPOR/CALR^del52
INCA033989
Isotype
TPOR
INCA033989
Isotype
B
UT-7 cells
GMFI
[Antibody] (μg/mL)
TPOR/CALR^del52
INCA033989
Isotype
TPOR
INCA033989
Isotype
C
pSTAT3 (Y705)
pSTAT5 (Y694)
pERK (T202/T204)
pCREB (S133)
pMEK1 (S298)
pAKT (S473)
pAKT (T308)
pmTOR (S2448)
mTOR
[IgG1] (μg/mL)
[INCA033989] (μg/mL)
Fold-change
D
Ba/F3-TPOR/CALR^del52
Inhibition of cell proliferation (%)
[Antibody] (μg/mL)
INCA033989
Isotype
E
UT-7-TPOR/CALR^del52
Inhibition of cell proliferation (%)
[Antibody] (μg/mL)
INCA033989
Isotype
F
Cells (%)
INCA033989
Dead
G0/G1
S
G2/M
IgG 100 μg
JAK2 V617F
mutCALR

Figure 1.

measured over time (Figure 2D). As these mice did not express mutCALR, no target-mediated drug disposition was observed. Maximum concentration in plasma was 59.8 μg/mL, with a terminal half-life of 128 hours. A volume of distribution of 130 mL/kg and clearance of 0.765 mL/h per kg (Figure 2D) indicated drug distribution to extravascular tissues and acceptable affinity to hFcRn in vivo.

As indicated above, the antagonistic ability of INCA033989 was not a result of receptor crosslinking. Furthermore, INCA033989 did not induce Fc-mediated immune effector function, which is in agreement with the Fc-silencing mutation of the antibody (Figure 2E-F). INCA033989 and a version of the antibody with wtIgG1-Fc did not induce complement-dependent cytotoxicity (CDC) in TF-1 cells expressing mutCALR (TF-1-TPOR/CALR-^{del52}). IgG1 and IgG4 versions of an anti-CD33 antibody were used as positive and negative controls for CDC, respectively (Figure 2E). Similarly, treatment of TF-1-TPOR/CALR^{del52} cells with INCA033989 or its wtIgG1-Fc counterpart did not trigger the activation of the FcγRIIIA reporter signal in effector cells, which is a surrogate for antibody-dependent cellular cytotoxicity (ADCC) function (Figure 2F). An anti-CD43 antibody and its respective Fc-silent version were used as the positive and negative controls (Figure 2F). Collectively, these data indicate that INCA033989 does not exert its antagonistic function via Fc-mediated CDC or ADCC.

INCA033989 antagonistic function is dependent on endocytosis of the mutCALR/TPOR complex

The mechanism of action of INCA033989 was further investigated using high-content imaging analysis. INCA033989 displayed time-dependent internalization in Ba/F3-TPOR/CALR^{del52} cells (Figure 3A). Importantly, no internalization of INCA033989 was observed in Ba/F3 cells that did not express mutCALR (data not shown). Endocytosis of INCA033989 was dynamin dependent because the presence of the dynamin inhibitor, dynasore, completely abrogated the internalization of INCA033989 (Figure 3B) and restored mutCALR-induced cell proliferation and inhibition of caspase activation (Figure 3C-D). Interestingly, dynasore treatment only partially restored the mutCALR-induced activation of pSTAT5 (Figure 3E).

Confocal microscopy confirmed the internalization of INCA033989 at 18 hours after cell treatment (Figure 3F). Additionally, the data showed that internalized INCA033989 colocalized with the lysosomal marker lysosome-associated membrane protein 2 (Figure 3G), suggesting that the INCA033989/mutCALR/TPOR complex is localized to the cell lysosome upon endocytosis and is likely targeted for degradation.

In agreement with these observations, flow cytometry, and confocal microscopy analyses confirmed INCA033989-induced internalization and degradation of TPOR in Ba/F3 and primary CD34$^+$ cells expressing mutCALR (supplemental Figure 5).

INCA033989 antagonizes mutCALR-induced oncogenic signaling and megakaryocyte differentiation of primary CD34$^+$ cells from patients with MPNs

To assess the functional impact of INCA033989 in primary cells of patients with MPNs, we confirmed selective mutCALR expression on the surface of peripheral blood mononuclear cells and CD34$^+$ HSPCs from patients with MF positive for the *CALR* mutation (Figure 4A-C).

INCA033989 selectively inhibited pSTAT3/pSTAT5 signaling in CD34$^+$ HSPCs from patients with MF positive for the *CALR* mutation but not in wt cells or cells from patients with mutations in *JAK2* or *MPL* (Figure 4D; supplemental Figure 6A). In contrast, the JAK1/2 inhibitor ruxolitinib equally inhibited pSTAT5 signaling in wt and MPN-derived CD34$^+$ cells, independent of the mutation status of the patient sample (supplemental Figure 6B).

Given the selectivity of INCA033989 for cells expressing mutCALR, we next investigated whether INCA033989 could inhibit pathogenic proliferation and differentiation of MPN CD34$^+$ cells without interfering with the wt cells. INCA033989 selectively prevented the proliferation of HSPCs expressing mutCALR in a dose-dependent manner, with no impact on wt cells (Figure 4E). Similarly, INCA033989 prevented the differentiation of mutCALR-expressing CD34$^+$ cells into mature megakaryocytes (Figure 4F). Notably, INCA033989 inhibited megakaryocyte differentiation of CD34$^+$ cells harboring either CALR^{del52} or CALR^{ins5} variants, whereas no impact was observed in CD34$^+$ cells carrying JAK2^{V617F} (Figure 4F).

Prolonged ex vivo treatment (>6 days) of CALR^{del52}-positive MPN-derived CD34$^+$ cells with INCA033989 at low dose demonstrated that the maximum antagonistic effect of the antibody was achieved after several days (Figure 4G). Internalization of INCA033989 was also confirmed in CALR^{del52}-positive MPN-derived CD34$^+$ cells by confocal microscopy (Figure 4H), in agreement with the endocytosis requirement for functional activity of INCA033989.

Together, these data show that INCA033989 acts as a functional antagonist of mutCALR-expressing CD34$^+$ cells and targets the abnormal proliferation of HSPCs and abnormal megakaryopoiesis induced by mutCALR.

Figure 1. INCA033989 antagonizes mutCALR-induced oncogenic signaling. (A-B) INCA033989 cell-binding profile. Binding of INCA033989 or isotype to Ba/F3-TPOR or Ba/F3-TPOR/CALR^{del52} (A) and UT-7-TPOR or UT-7-TPOR/CALR^{del52} (B) cells was assessed by flow cytometry (see supplemental Methods for details). The data represent the GMFI of 3 independent experiments. (C) INCA033989 antagonizes mutCALR-induced oncogenic signaling. Ba/F3-TPOR/CALR^{del52} cells treated with increasing concentrations of INCA033989, isotype, or vehicle for 4 hours were barcoded, stained with phospho-specific antibodies, and evaluated using flow cytometry. The heat maps show mean fluorescence intensity from n = 3 independent experiments. The color scale represents the fold change over untreated Ba/F3-TPOR cells (baseline). (D-E) INCA033989 antagonizes mutCALR-induced oncogenic cell proliferation. Ba/F3-TPOR/CALR^{del52} (D) and UT-7-TPOR/CALR^{del52} (E) cells were treated with INCA033989 or isotype for 72 hours and cell proliferation was assessed. Inhibition of cell proliferation was calculated after normalization to maximal (100%) inhibition achieved by cell treatment with 2 to 5 μM of ruxolitinib and no inhibition (0%) in isotype-treated cells. The data are representative of 3 independent experiments. (F) INCA033989 induces the death of mutCALR-positive cells. Ba/F3-EPOR/JAK2^{V617F} and Ba/F3-TPOR/CALR^{del52} cells were treated with INCA033989 or isotype for 48-hours pulse labeled with 5-bromo-2'-deoxyuridine and stained with 7-Aminoactinomycin for cell cycle evaluation by flow cytometry (see supplemental Methods for details). Data represent the mean of triplicates ± SD and are representative of 2 independent experiments. AKT, protein kinase B; CREB, cyclic adenosine monophosphate responsive element binding protein; ERK, extracellular signal–regulated kinase; GMFI, geometric mean of fluorescence intensity; mTOR, mammalian target of rapamycin; SD, standard deviation.

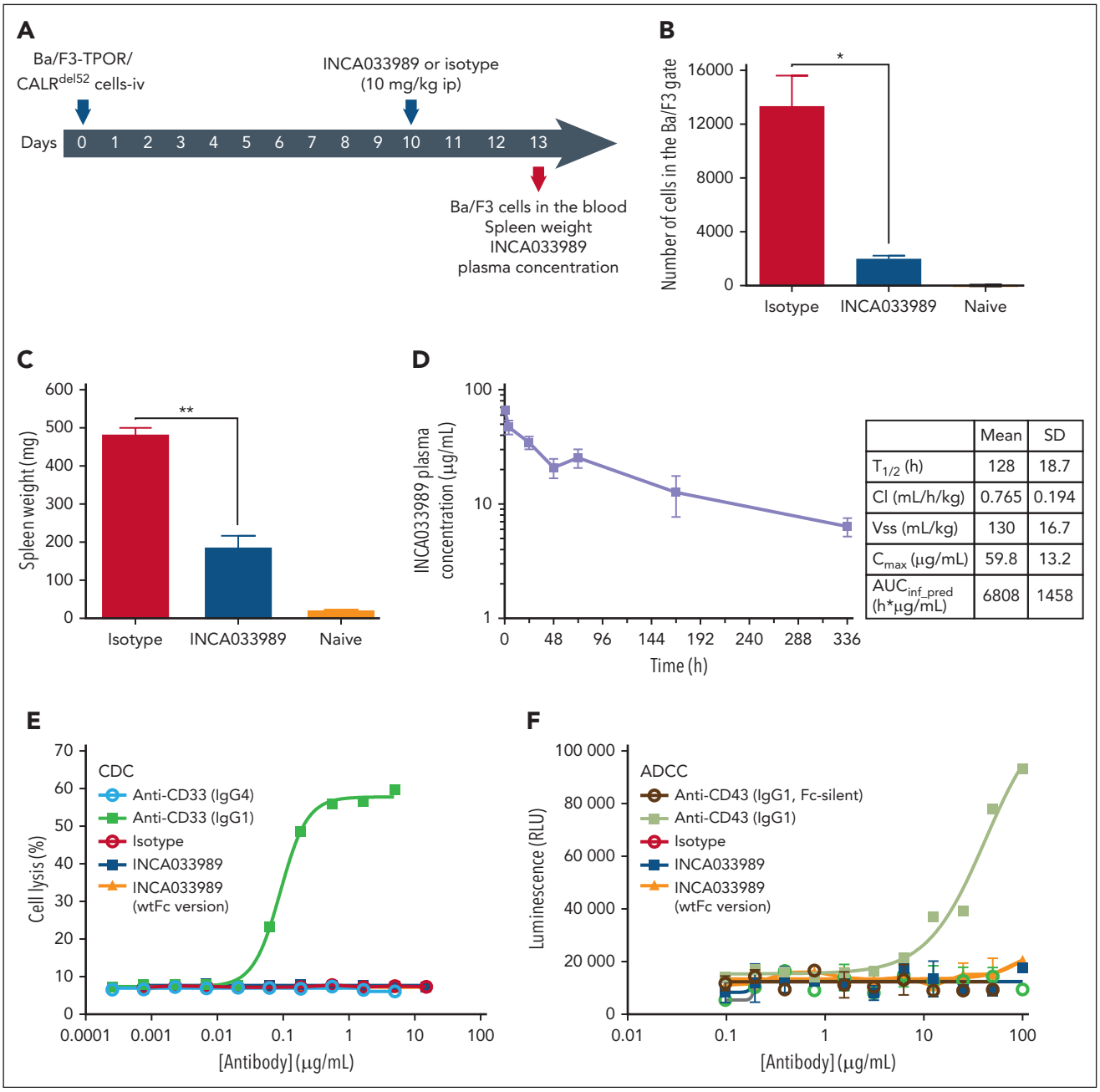

Figure 2. INCA033989 antagonizes mutCALR-dependent cell proliferation in vivo. (A) Study schematic. NSG mice (n = 4 per group) were inoculated IV with 20 000 Ba/F3-TPOR/CALR^{del52} cells. A single 10-mg/kg intraperitoneal dose of INCA033989 or isotype was administered on day 10 after cell inoculation. The number of Ba/F3 cells in the blood, spleen size, and drug exposure were monitored on day 13 (3 days after a single injection of INCA033989). Noninoculated untreated NSG-naive mice were used as controls (see supplemental Methods for details). (B) Relative numbers of Ba/F3 cells in a sample of whole blood. (C) Spleen weight. Data are presented as the mean ± standard error of the mean (SEM; n = 4 mice per group). Significance was calculated using a parametric *t* test. *$P < .05$; **$P < .01$. (D) INCA033989 PK in hFcRn mice. Mice (n = 4) were dosed IV with 5 mg/kg of INCA033989, the drug concentration was measured in the plasma over time, and PK parameters were calculated. (E) INCA033989 does not induce CDC. TF-1-TPOR/CALR^{del52} cells were treated with INCA033989 and other control antibodies for 4 hours in the presence of 5% baby rabbit serum for assessment of cell cytotoxicity. Digitonin (10%) was used as the positive control for cell lysis. The graph shows representative results from 3 independent experiments. (F) INCA033989 does not induce ADCC. Jurkat FcγIIIA reporter effector cells and TF-1-TPOR/CALR^{del52} cells (4:1 effector-to-target cell ratio) were treated with INCA033989 and other control antibodies for 24 hours for assessment of FcγIIIA engagement. The graph depicts a representative of 3 independent experiments (See supplemental Methods for further details). ADCC, antibody-dependent cellular cytotoxicity; AUC, area under concentration-time curve; Cl, clearance; C_{max}, maximum observed plasma concentration; ip, intraperitoneal; RLU, relative light units; $T_{1/2}$, half-life; Vss, steady-state volume of distribution.

INCA033989 mouse surrogate antibody induces hematologic and molecular effects in a *CALR*^{del52} mouse model of MPN

To explore the efficacy of INCA033989 in a disease-relevant format, we used a mouse model that resembles the molecular and cellular phenotypes of clinical ET. The model consists of a competitive transplantation of 20% CALR$^{del52/del52}$ LoxP/SCL-Cre-ER^{T} and 80% of wt/GFP^{+} bone marrow cells in lethally irradiated mice.[21] Two weeks after CALR$^{del52/del52}$ induction with tamoxifen, blood parameters, and mutCALR

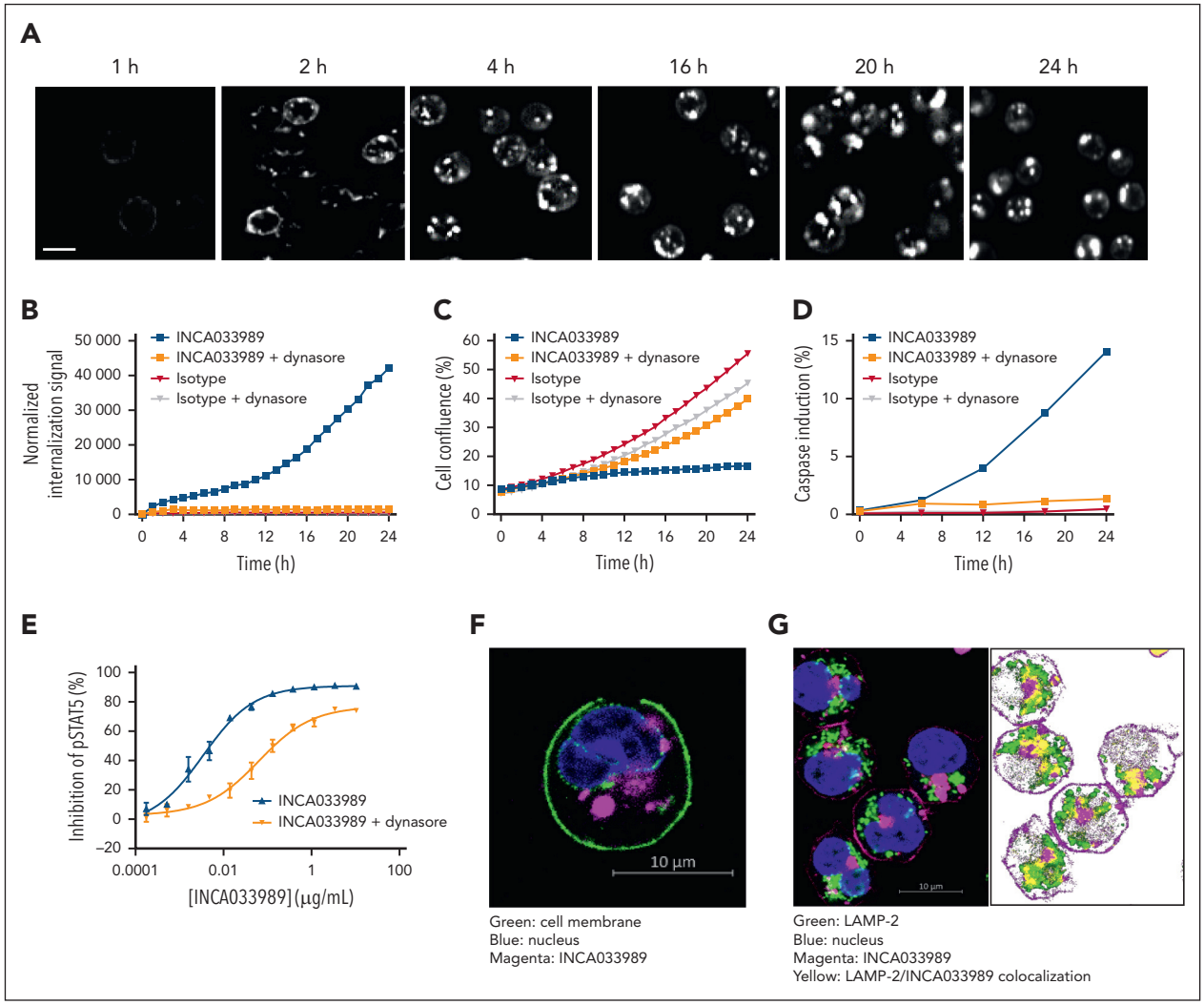

Figure 3. INCA033989 antagonistic effect is dependent on cell internalization. (A) Time-dependent binding of Alexa Fluor 647–INCA033989 to Ba/F3-TPOR/CALR^{del52} cells, measured using high-content imaging. Representative images are shown at a 20× magnification. Scale bar = 10 µm. (B-D) Ba/F3-TPOR/CALR^{del52} cells were pre-incubated for 10 minutes with dynasore or dimethyl sulfoxide (DMSO), followed by treatment with Fabfluor-labeled INCA033989 or -isotype for 24 hours (see supplemental Methods for further details). (B) Internalization rate of Fabfluor-pH sensitive–labeled antibodies over time. (C) Cell proliferation over time, calculated as the cell confluence. (D) Caspase induction over time. (E) Ba/F3-TPOR/CALR^{del52} cells were treated with INCA033989 premixed with dynasore (inhibitor of dynamin-dependent endocytosis) or DMSO and incubated for 3 hours and levels of pSTAT5 were assessed by Meso Scale Discovery. Inhibition of pSTAT5 was calculated after normalization to the maximal (100%) inhibition achieved by the cell treatment with 6 µM of ruxolitinib and no inhibition (0%) in DMSO-treated cells. The data are representative of 3 independent experiments. (F) INCA033989 is internalized upon binding to mutCALR on the cell surface. Ba/F3-TPOR/CALR^{del52} cells were treated with Alexa Fluor 647–INCA033989 for 18 hours and the microscopy images were evaluated. Green: cell membrane; blue: nucleus; magenta: INCA033989. (G) INCA033989 colocalizes with lysosomal markers upon internalization. Ba/F3-TPOR/CALR^{del52} cells were pretreated with Alexa Fluor 647–INCA033989 for 2 hours on ice, followed by washing and additional incubation for 6 hours at 37°C. The lysosomal compartment was stained with anti-LAMP-2 and the cells were evaluated by microscopy. Green: LAMP-2; blue: nucleus; magenta: INCA033989; yellow: colocalization of LAMP-2 and INCA033989. LAMP-2, lysosome-associated membrane protein 2.

chimerism were assessed. Mice were randomized and treated with either an isotype control or a mouse surrogate version of INCA033989 (10 mg/kg) twice a week for 10 weeks (supplemental Figure 7A).

As previously demonstrated,[21] mice treated with isotype IgG progressively developed thrombocytosis, with platelet counts reaching 2500 × 10^3 cells per µL after 10 weeks of tamoxifen induction, as well as mild leukocytosis (Figure 5A; supplemental Figure 7B-C). In contrast, treatment with the INCA033989 mouse surrogate prevented thrombocytosis, with platelet counts remaining within normal range while not impacting white blood cells or hemoglobin (Figure 5A; supplemental Figure 7B-C). mutCALR chimerism started at 50% to 60% in platelets and <30% in red blood cells and granulocytes, and gradually increased over time in all blood cell types in the isotype control–treated mice (Figure 5B; supplemental Figure 7D-E). In contrast, the INCA033989 mouse surrogate considerably inhibited the expansion of mutCALR-positive platelets (96% vs 36%), red blood cell, and granulocytes, suggesting the selective targeting of HSCs that are positive for mutCALR (Figure 5B; supplemental Figure 7D-E). These results indicate that the INCA033989 mouse surrogate induces both hematologic and molecular responses by targeting mutCALR-positive cells in favor of wt blood cells.

Analysis of the bone marrow HSC and HSPC compartments after 10 weeks of treatment indicated that mutCALR cells

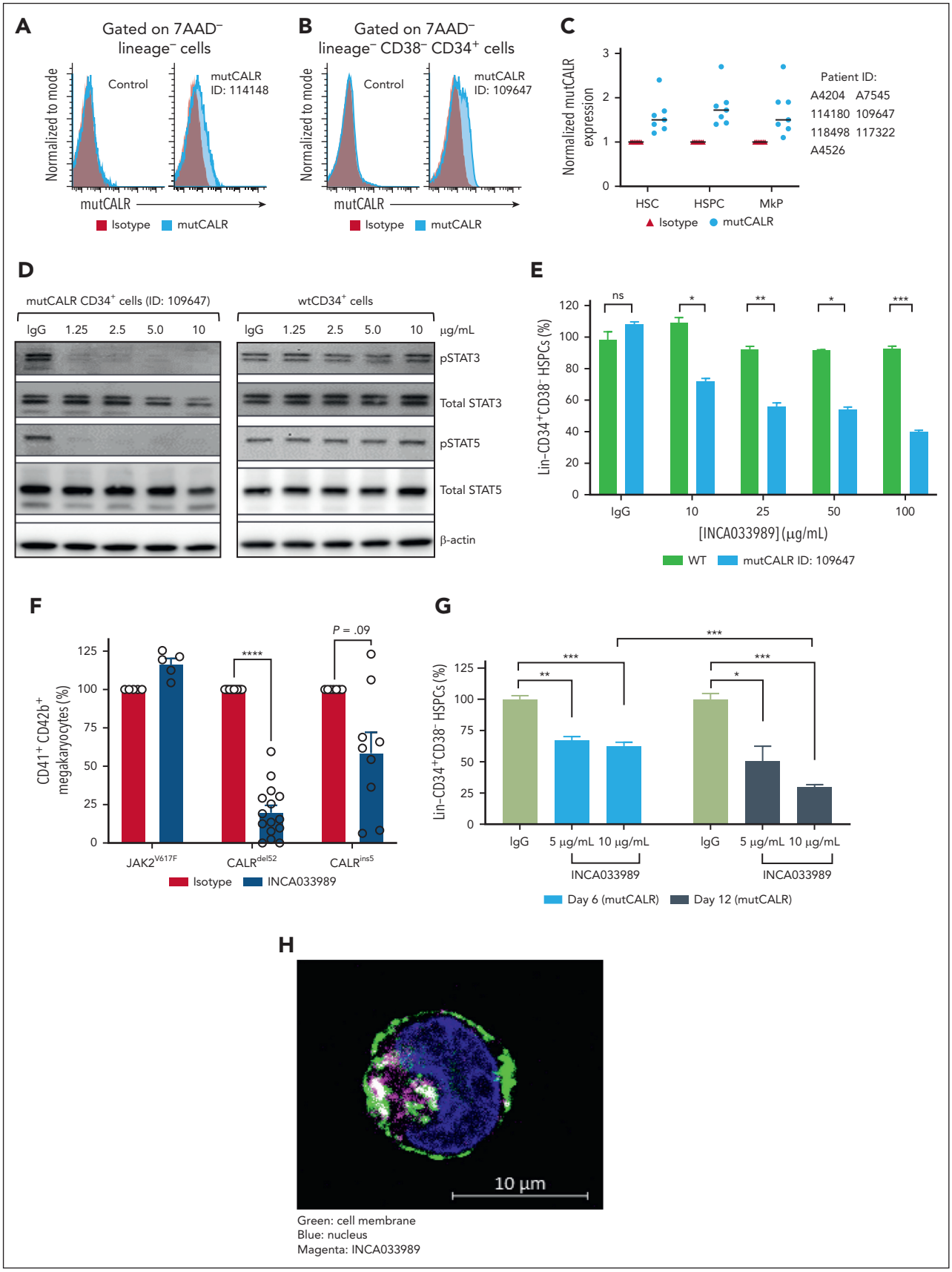

Figure 4. INCA033989 antagonizes mutCALR-induced oncogenic signaling and megakaryocyte differentiation in primary CD34⁺ patient cells. (A-C) A subpopulation of CD34⁺ cells isolated from mutCALR-positive patients with MF express mutCALR. (A) Representative flow cytometric analysis of the Lin⁻ peripheral blood mononuclear cells from a healthy individual (control) or a CALR^{del52} patient with MF (mutCALR). (B) Flow cytometric analysis of Lin⁻CD34⁺CD38⁻ cells from a healthy individual (control) and a

outcompeted normal wt cells in bone marrow, reaching ~90% in the signaling lymphocyte activation molecule compartment (Figure 5C), as previously demonstrated.[21] Treatment with the INCA033989 mouse surrogate reduced the number of mutCALR-positive bone marrow progenitors and stem cells, including long-term HSCs (LT-HSCs; 85% vs 32%; Figure 5C) as well as mutCALR-positive erythroblastic and granulocytic precursors (supplemental Figure 7F). Additionally, the frequencies of mutCALR-positive megakaryocytic progenitors and megakaryocytes were significantly lower in mice treated with the INCA033989 mouse surrogate when compared with isotype control–treated counterparts (supplemental Figure 7G), consequently leading to normalization of bone marrow histology showing normal numbers of megakaryocytes (Figure 5D). Notably, despite a reduction in the number of mutCALR-positive cells, the overall bone marrow cellularity was not impacted by the INCA033989 mouse surrogate (supplementary Figure 7H), in agreement with the selective targeting of mutant cells without affecting normal hematopoiesis. Additionally, no weight loss after INCA003989 treatment (supplemental Fig 7I) and no change in spleen architecture were observed 10 weeks after treatment initiation (supplemental Fig 7J), indicating a favorable safety profile.

To assess whether the INCA033989 mouse surrogate could target disease-initiating stem cells, disease relapse was evaluated after treatment arrest. Although thrombocytosis was persistent in isotype control–treated mice, platelet counts remained within the normal range (830×10^3 to 1130×10^3 cells per μL) during the first 7 weeks after the arrest of INCA033989 mouse surrogate antibody treatment (Figure 5E-F).

Secondary transplantations were performed with the bone marrow of mice that had been treated with isotype control or INCA033989 mouse surrogate for 10 weeks. Although mice engrafted with bone marrow cells from the isotype control–treated mice developed thrombocytosis, along with a significant increase in mutCALR chimerism in the blood (Figure 5G-H), mice engrafted with cells from INCA033989 mouse surrogate–treated mice did not develop thrombocytosis and showed reduced levels of mutCALR-positive platelets (Figure 5G-H). Altogether, these results indicate that the INCA033989 mouse surrogate restores normal hematopoiesis by selectively targeting mutCALR cells, including LT-HSCs, which are considered disease-initiating cells responsible for disease initiation and maintenance.

Discussion

In this article, we describe INCA033989 as the first mutCALR-targeted therapy to enter clinical trials for the treatment of MF and ET (ClinicalTrials.gov identifiers: NCT05936359 and NCT06034002). INCA033989 shows selective targeting of mutCALR and potent antagonism of mutCALR-induced oncogenic signaling. Our in vitro and in vivo data strongly support the selective targeting of mutCALR-positive disease-initiating cells by INCA033989 without affecting normal hematopoiesis.

It has been 10 years since mutCALR was first uncovered as a driver of ET and MF in 80% of patients with MPNs who are negative for mutations in *JAK2* or *MPL*.[2,3] After this discovery, significant progress has been made toward understanding the oncogenic role of mutCALR, including interaction with TPOR in the ER, trafficking of the mutCALR/TPOR complex to the cell surface, abnormal JAK/STAT activation, and association with MPNs.[5-11,14,25-27] Such findings fueled interest in targeted therapeutics against the mutCALR neoepitope and as a result, vaccines and antibody therapies are currently being investigated.[28,29] Cell surface localization of mutCALR makes it an attractive target for antibodies and preclinical studies have been reported. CAL2, a monoclonal antibody generated via immunization of mice with a 22 amino acid peptide derived from the mutCALR C-terminus, selectively stains megakaryocytes in bone marrow sections of mutCALR-positive patients with MPN, showing potential for diagnostic use.[30] Preclinical studies using rat and mouse monoclonal antibodies have shown that these mutCALR antibodies suppress thrombocytosis in in vivo mouse models of ET.[31,32] No further information regarding the mechanism of action or further development of these antibodies has been reported. An additional rat monoclonal antibody, 4D7, was reported to act as an antagonist and inhibit TPO-independent megakaryocyte differentiation of cells from patients with MPN positive for mutCALR and prolong survival of mice injected with cell lines expressing mutCALR in an in vivo xenograft model.[33]

The antibodies described above do not have their mechanism of action well characterized and/or were raised in nonhuman species, with a potential risk of immunogenicity in humans. In contrast, INCA033989 is a fully human IgG1 monoclonal antibody with antagonistic activity and drug-like PK properties, with a clear potential for therapeutic use. INCA033989 does not induce Fc-mediated activation of immune cells, thereby avoiding potential immune-mediated adverse events.[34,35] Interestingly, a variant of INCA033989 with wtIgG1-Fc was also unable to induce Fc-mediated functions, suggesting that low cell surface expression of mutCALR likely limits the ability of anti-mutCALR antibodies to induce Fc-mediated immune effector function against MPN cells. Indeed, previous reports indicate that target expression levels and accessibility are key factors determining the potency of the Fc-mediated effector function of an antibody.[36] In line with these observations, data

Figure 4 (continued) patient with MF (mutCALR). (C) Normalized mutCALR signal intensity in $Lin^-/CD34^+/CD38^-/CD45Ra^-/CD90^+$ HSCs, $Lin^-/CD34^+/CD38^-$ HSPCs, and $Lin^-/CD34^+/CD41^+$ MkPs from 7 patients with MF (mutCALR). (D) Western blot analysis of $CD34^+$ cells isolated from a patient with MF (mutCALR) or from human cord blood from a healthy individual ($wtCD34^+$) treated with different concentrations of INCA033989 or an IgG control (10 μg/mL). pSTAT3/5 expression was induced by TPO (50 ng/mL) in $wtCD34^+$ cells. (E-G) $CD34^+$ progenitor cells from a healthy individual (wt) or patients with MF carrying the $JAK2^{V617F}$ or *CALR* mutations were cultured in stem cell factor alone or the presence of the indicated concentrations of INCA033989 or control IgG (10 μg/mL) for 6 days. The impact of INCA033989 on $CD34^+$-derived cell populations was assessed by flow cytometry. Significance was calculated using analysis of variance (ANOVA). $^*P < .05$; $^{**}P < .01$; $^{***}P < .001$; $^{****}P < .000001$. Percentages of wt and mutCALR $Lin^-/CD34^+/CD38^-$ HSPCs. (E) Representative data from cells from a single patient. (F) $JAK2^{V617F}$ (n = 5), $CALR^{del52}$ (n = 15), and $CALR^{ins5}$ (n = 9) megakaryocytes after treatment with 10 or 25 μg/mL of isotype or INCA033989. (G) Percentages of mutCALR $Lin^-/CD34^+/CD38^-$ HSPCs after 6 and 12 days of INCA033989 treatment. (H) INCA033989 is internalized upon the binding of mutCALR to the surface of primary $CD34^+$ cells. $CD34^+$ cells from a mutCALR-positive patient with MF were treated with 2 μg/mL of AF647-labeled INCA033989 for 18 hours, prepared for microscopy, and evaluated using the ZEN software suite. Green: cell membrane; blue: nucleus; magenta: INCA033989. Lin, lineage; MkP, megakaryocyte progenitor; ns, not significant.

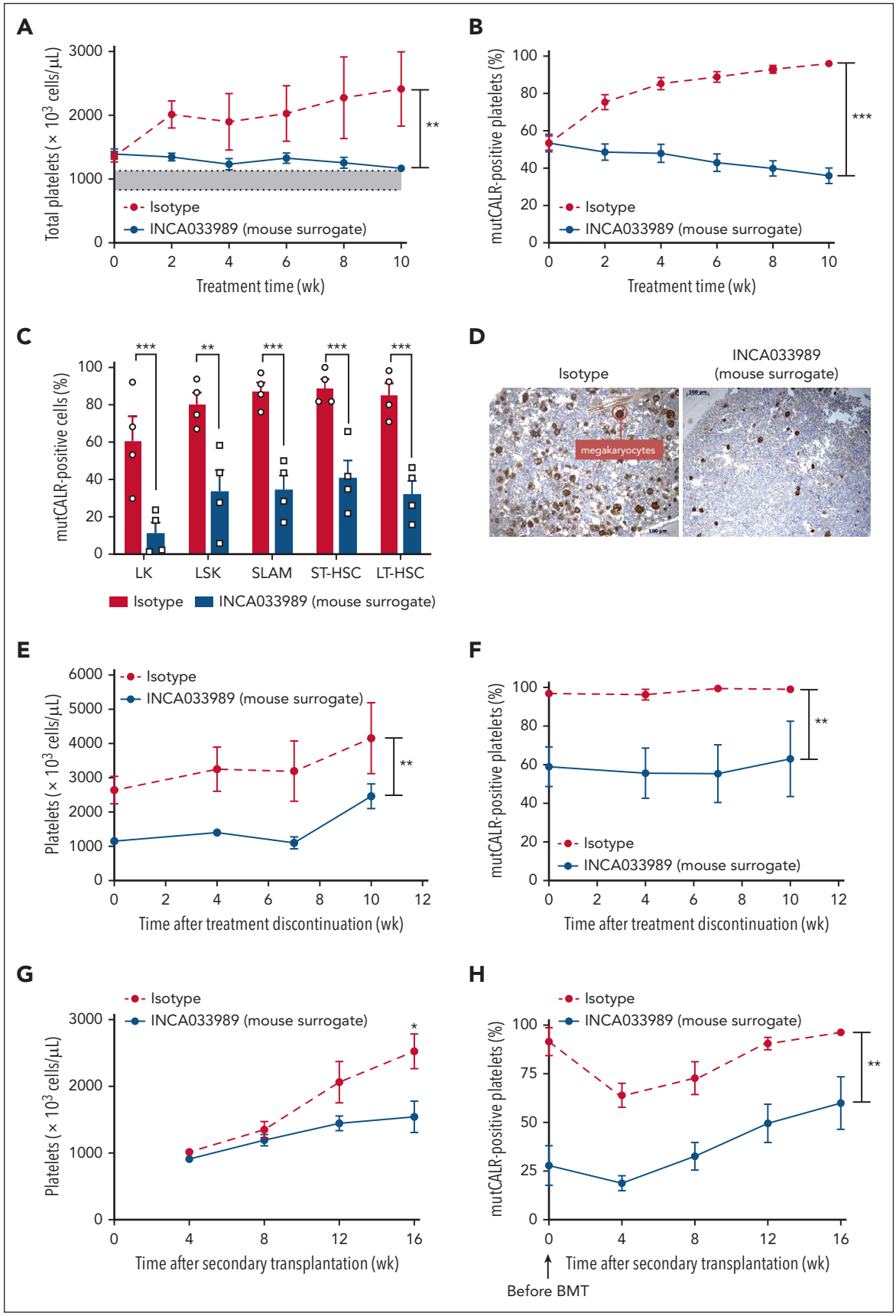

Figure 5. INCA033989 mouse surrogate induces hematologic and molecular effects in the blood and bone marrow by targeting disease-initiating stem cells. A preclinical mouse model with competitive transplantation using 20% of *CALR*$^{del52/del52}$ LoxP/SCL-Cre-ER^{T} bone marrow cells and 80% of wt/GFP^{+} bone marrow cells. Two

from an in vivo mouse model of MPN indicated similar therapeutic efficacy between INCA033989 and an equivalent mut-CALR antibody with a wtIgG1-Fc (data not shown).

The mechanism of mutCALR antagonism with INCA033989 was determined to be partially through dynamin-dependent endocytosis of the INCA033989/mutCALR/TPOR complex. The data indicate that antagonism of the oncogenic function of MPN cells with INCA033989 is decreased upon inhibition of the dynamin-dependent endocytosis pathway.[37] TPO-induced TPOR internalization and TPOR recycling or lysosomal degradation have been previously reported.[38,39] However, further investigation is required to understand if and how mutCALR itself or the binding of INCA033989 to the mutCALR/TPOR complex affects the TPOR recycling process. Notably, although endocytosis is required for the antagonistic function of INCA033989, internalization of the INCA033989/mutCALR/TPOR complex is only partially responsible for INCA033989-mediated inhibition of pSTAT5. Because INCA033989-mediated pSTAT5 inhibition is an early event (maximum inhibition observed in 2 hours), it is likely that binding of INCA033989 to mutCALR/TPOR on the cell surface disturbs the conformational structure of the complex, leading to rapid JAK/STAT inhibition, followed by slower internalization of the complex. More detailed characterization of this mechanism of action will require a better understanding of the dynamics of spatial and conformational properties of the TPOR/mutCALR complex.[10]

SPR data suggest a slightly preferential binding of INCA033989 to CALR^{del52} when compared with CALR^{ins5}, which is consistent with the superior potency of INCA033989 in CALR^{del52} MPN cells relative to CALR^{ins5} cells. Interestingly, data from a recent study on the requirements for TPOR/mutCALR complex formation suggest that the same amino acid residues are involved in the TPOR/mutCALR interaction, independent of whether CALR^{del52} or CALR^{ins5} are present.[10] In contrast, multiple sources of evidence suggest that type 1 and 2 mutations result in differential signaling and disease phenotypes.[6,12,27,40,41] In an attempt to reconcile the observations above, we hypothesize that the differential signaling induced by CALR^{del52} and CALR^{ins5} and preferential activity of INCA033989 in type 1 cells are likely a consequence of a distinct tertiary structure of the TPOR-CALR^{del52} complex when compared with that of TPOR-CALR^{ins5}; that is, the epitope for INCA033989 is more exposed in the TPOR-CALR^{del52} complex. Additional structural understanding of the mutCALR-TPOR complex is warranted to better delineate the molecular and functional differences between CALR^{del52} and CALR^{ins5,} and the consequent impact on the function of INCA033989.

Current therapeutic approaches used to treat patients with MPNs are independent of the MPN driver mutation (ie, *CALR*, *JAK2*, *MPL*, or triple negative) and are decided based on patient risk stratification.[42] For MF, in particular, bone marrow stem cell transplantation is the only treatment with curative potential but is associated with risks such as severe morbidity and death.[13,43] The therapeutic landscape for MF includes androgens, immunosuppressors, hydroxyurea, and JAK inhibitors (ruxolitinib, fedratinib, momelotinib, and pacritinib), and patients with ET are managed with aspirin, cytoreduction, hydroxycarbamine, or peginterferon.[17-20] Although these alternatives assist with symptom relief and splenomegaly, they are associated with intolerance and resistance, that may lead to drug discontinuation. Further, ~10% of patients with ET will progress to MF,[44] the more severe form of MPNs, and mutCALR-positive patients with ET appear to be less sensitive to interferon therapy and more likely to develop drug resistance.[19,45,46]

The scenario laid out above is partially a consequence of non-targeted therapies that affect both mutated and nonmutated cells and their inefficacy in eliminating the cause of the disease (ie, HSCs and HSPCs expressing oncogenic mutations).[20] INCA033989 demonstrates the potential to be a disease-modifying agent given its ability to selectively target mutCALR-positive disease-initiating cells. The disease-modifying potential of INCA033989 is supported by data from CD34$^+$ cells derived from mutCALR-positive patients with MPN and the MPN mouse model. INCA033989 treatment of CD34$^+$ cells from mutCALR-positive patients with MPN resulted in decreased proliferation of HSPCs and megakaryocyte differentiation. The inhibition of mutCALR-induced oncogenic signaling by INCA033989 leads to the death of mutCALR-positive cells without affecting normal cells that continue to proliferate. The decrease in the megakaryocytic population is likely a consequence of the direct targeting of megakaryocytes, megakaryocyte progenitors, and early HSCs.[47,48] The selective targeting of mutCALR-positive LT-HSCs by INCA033989, as observed in the MPN in vivo model, supports the potential of INCA033989 to eliminate disease-initiating cells and rescue normal hematopoiesis. Given its mechanism of action and safety profile, we hypothesize that INCA033989 will show potent therapeutic effects both in patients with ET and patients with MF and early-stage disease. It remains to be determined whether the antibody as a single agent can revert the disease status in patients with late-stage MF with highly fibrotic bone marrow and multiple concurrent mutations. Possibly, longer treatment periods and combination therapies are required for these patients.

Figure 5 (continued) weeks after *CALR*$^{del52/del52}$ induction, blood parameters and chimerism were assessed, and the mice were randomized. Mice were treated with isotype or INCA033989 mouse surrogate (10 mg/kg) twice a week, and the hematologic and molecular responses were assessed every 2 weeks for 10 weeks. (A) Platelet counts measured in blood. The gray area depicts the normal range of platelet counts. Data are presented as mean ± SEM (n = 6 mice per group). Significance was calculated using a parametric *t* test with Welch correction. ***P* < .01. (B) mutCALR chimerism was monitored by flow cytometry in platelets (CD41$^+$). Data are presented as mean ± SEM (n = 6 mice per group). Significance was calculated by parametric *t* test with Welch correction. ****P* < .001. (C-D) Bone marrow evaluation at 10 weeks after treatment initiation. (C) The bone marrow was analyzed for mutCALR chimerism in progenitors by flow cytometry using a GFP marker. Data are presented as the mean ± SEM (n = 4 mice per group). Significance was determined using 2-way ANOVA with the Tukey multiple comparison test. (D) Pictures represent the histopathological analyses of bone marrow from 1 out of 4 mice per group treated with isotype or INCA033989 mouse surrogate after von Willebrand factor staining. (E-F) Relapse study in mice treated with IgG or INCA033989 mouse surrogate for 10 weeks, in which treatment was discontinued during the following 10 weeks. Platelet counts (E) and proportion of mutCALR-positive platelets (F) are shown. Data are mean ± SEM (n = 4 mice per group). Significance was calculated by parametric *t* test with Welch correction. ***P* < .01. (G-H) Secondary engraftments were performed with bone marrow cells isolated from mice treated with IgG or INCA033989 mouse surrogate, and the platelet counts (G) and platelet chimerism (H) were followed without any treatment over 16 weeks. Data are presented as the mean ± SEM (n = 10 mice per group from 2 donor mice). Significance was calculated by parametric *t* test with Welch correction. **P* < .05; ***P* < .01. BMT, bone marrow transplant; LK, Lin$^-$Sca$^+$; LSK, Lin$^-$Sca$^+$Kit$^+$; LT-HSC, long-term HSC; SLAM, signaling lymphocyte activation molecule; ST-HSC, short-term HSC.

Overall, this study shows the characterization of INCA033989, the first mutCALR oncogene–targeted therapy developed for patients with MPNs. This monoclonal antibody shows the potential to change the disease course in patients with MPN harboring *CALR* mutations, and a phase 1 clinical trial is underway.

Acknowledgments

The authors thank Shireen Shaikh and Niketa Langalia from the Antibody Discovery Division at Incyte for excellent assistance with the antibody discovery campaigns. The authors also thank Karen Hogg from the Imaging and Cytometry Laboratory of the University of York Bioscience Technology Facility for assistance with the fluorescent cell barcoding and phospho-flow cytometry and Daniel Yee for generating the UT-7 TPO cell lines. Editorial assistance and graphics support were provided by the Envision Pharma Group (Philadelphia, PA) and funded by the Incyte Corporation.

This work was supported by the Ligue Nationale contre le Cancer (équipe labellisée 2019), Institut Nacional du Cancer PLBIO 2021, and Inserm (to C.M., E.R., M.E, W.V., and I.P.).

Authorship

Contribution: E.S.R., C.M., S.S., I.S.H., D. Dhanak, R.M., I.P., H.N., and P.A.M. designed and performed research, analyzed and interpreted data, and wrote the manuscript; R.B. and H.C. designed and performed research, collected data, analyzed and interpreted data, and wrote the manuscript; A.L., F.J., M.R., Y.Z., D. DiMatteo, R.A., B.L.F., L. Leffet, L. Lu, G.T., E.R., M.E., B.W., A.H., X.H., and A.V. performed research, collected data, analyzed and interpreted data, and wrote the manuscript; M.C., W.V., Y.-o.Y., B.B., and J.Z. performed research, analyzed and interpreted data, and wrote the manuscript; and F.P., G.F., and L. Legros contributed vital reagents and wrote the manuscript.

Conflict-of-interest disclosure: E.S.R., R.B., H.C., F.J., M.R., Y.Z., D. DiMatteo, R.A., L. Leffet, L. Lu, G.T., B.W., A.H., X.H., M.C., A.V., Y.-o.Y., B.B., R.M., H.N., and P.A.M. are employees of and own stock at the Incyte Corporation. A.L., J.Z., S.S., and D. Dhanak are former employees of and own stock at the Incyte Corporation. C.M., B.L.F., E.R., M.E., W.V., I.S.H., and I.P. received research funding from Incyte Corporation. L. Legros received research funding from Incyte Corporation; a travel grant from Novartis and Pfizer; and is on advisory boards for Amgen, Bristol Myers Squibb, GlaxoSmithKline, Incyte Corporation, Novartis, and Pfizer. The remaining authors declare no competing financial interests.

ORCID profiles: R.B., 0000-0002-8158-8074; C.M., 0000-0003-4350-2302; D.D., 0000-0003-3440-3724; F.P., 0000-0003-1432-5300; G.F., 0000-0002-3751-393X; W.V., 0000-0003-4705-202X; Y.-o.Y., 0009-0005-4869-9492; S.S., 0000-0001-7915-9193; I.S.H., 0000-0001-7170-6703; R.M., 0000-0001-8868-2146; I.P., 0000-0002-5915-6910; P.A.M., 0000-0001-9104-4161.

Correspondence: Edimara S. Reis, Incyte Corporation, 1801 Augustine Cut-Off, Wilmington, DE 19803; email: ereis@incyte.com; and Patrick A. Mayes, Incyte Corporation, 1801 Augustine Cut-Off, Wilmington, DE 19803; email: pmayes@incyte.com.

Footnotes

Submitted 28 February 2024; accepted 30 August 2024; prepublished online on *Blood* First Edition 10 September 2024. https://doi.org/10.1182/blood.2024024373.

All data generated and analyzed during this study are included in this article and the supplemental data available with the online version of the article. Any additional data requests or inquiries should be directed to the corresponding authors, Edimara S. Reis (ereis@incyte.com) and Patrick A. Mayes (pmayes@incyte.com).

The online version of this article contains a data supplement.

There is a *Blood* Commentary on this article in this issue.

The publication costs of this article were defrayed in part by page charge payment. Therefore, and solely to indicate this fact, this article is hereby marked "advertisement" in accordance with 18 USC section 1734.

REFERENCES

1. Morsia E, Torre E, Poloni A, Olivieri A, Rupoli S. Molecular pathogenesis of myeloproliferative neoplasms: from molecular landscape to therapeutic implications. *Int J Mol Sci*. 2022;23(9):4573-4591.
2. Klampfl T, Gisslinger H, Harutyunyan AS, et al. Somatic mutations of calreticulin in myeloproliferative neoplasms. *N Engl J Med*. 2013;369(25):2379-2390.
3. Nangalia J, Massie CE, Baxter EJ, et al. Somatic *CALR* mutations in myeloproliferative neoplasms with nonmutated *JAK2*. *N Engl J Med*. 2013;369(25):2391-2405.
4. El Jahrani N, Cretin G, de Brevern AG. CALR-ETdb, the database of calreticulin variants diversity in essential thrombocythemia. *Platelets*. 2022;33(1):157-167.
5. Chachoua I, Pecquet C, El-Khoury M, et al. Thrombopoietin receptor activation by myeloproliferative neoplasm associated calreticulin mutants. *Blood*. 2016;127(10):1325-1335.
6. Marty C, Pecquet C, Nivarthi H, et al. Calreticulin mutants in mice induce an MPL-dependent thrombocytosis with frequent progression to myelofibrosis. *Blood*. 2016;127(10):1317-1324.
7. Araki M, Yang Y, Masubuchi N, et al. Activation of the thrombopoietin receptor by mutant calreticulin in CALR-mutant myeloproliferative neoplasms. *Blood*. 2016;127(10):1307-1316.
8. Elf S, Abdelfattah NS, Chen E, et al. Mutant calreticulin requires both its mutant C-terminus and the thrombopoietin receptor for oncogenic transformation. *Cancer Discov*. 2016;6(4):368-381.
9. Elf S, Abdelfattah NS, Baral AJ, et al. Defining the requirements for the pathogenic interaction between mutant calreticulin and MPL in MPN. *Blood*. 2018;131(7):782-786.
10. Papadopoulos N, Nedelec A, Derenne A, et al. Oncogenic CALR mutant C-terminus mediates dual binding to the thrombopoietin receptor triggering complex dimerization and activation. *Nat Commun*. 2023;14(1):1881-1896.
11. Pecquet C, Chachoua I, Roy A, et al. Calreticulin mutants as oncogenic rogue chaperones for TpoR and traffic-defective pathogenic TpoR mutants. *Blood*. 2019;133(25):2669-2681.
12. Pietra D, Rumi E, Ferretti VV, et al. Differential clinical effects of different mutation subtypes in *CALR*-mutant myeloproliferative neoplasms. *Leukemia*. 2016;30(2):431-438.
13. Szuber N, Tefferi A. Driver mutations in primary myelofibrosis and their implications. *Curr Opin Hematol*. 2018;25(2):129-135.
14. How J, Hobbs GS, Mullally A. Mutant calreticulin in myeloproliferative neoplasms. *Blood*. 2019;134(25):2242-2248.
15. US Food and Drug Administration. FDA approves first drug to treat a rare bone marrow disease. Press release. 16 November 2011. Accessed 12 January 2024. https://web.archive.org/web/20130128163618/http://www.fda.gov/NewsEvents/Newsroom/PressAnnouncements/ucm280102.htm
16. US Food and Drug Administration. FDA approves Jakafi to treat patients with a chronic type of bone marrow disease: first FDA-approved drug for polycythemia vera. Press release. 4 December 2014. Accessed 12 January 2024. https://wayback.archive-it.org/7993/20170111160849/http://www.fda.gov/NewsEvents/Newsroom/PressAnnouncements/ucm425677.htm

17. Waksal JA, Mascarenhas J. Novel therapies in myelofibrosis: beyond JAK inhibitors. *Curr Hematol Malig Rep*. 2022;17(5):140-154.

18. Yilmaz M, Verstovsek S. Managing patients with myelofibrosis and thrombocytopenia. *Expert Rev Hematol*. 2022;15(3):233-241.

19. Godfrey AL, Green AC, Harrison CN. Essential thrombocythemia: challenges in clinical practice and future prospects. *Blood*. 2023;141(16):1943-1953.

20. How J, Garcia JS, Mullally A. Biology and therapeutic targeting of molecular mechanisms in MPNs. *Blood*. 2023;141(16):1922-1933.

21. Benlabiod C, Cacemiro MDC, Nedelec A, et al. Calreticulin del52 and ins5 knock-in mice recapitulate different myeloproliferative phenotypes observed in patients with MPN. *Nat Commun*. 2020;11(1):4886-4900.

22. Göthert JR, Gustin SE, Hall MA, et al. In vivo fate-tracing studies using the *Scl* stem cell enhancer: embryonic hematopoietic stem cells significantly contribute to adult hematopoiesis. *Blood*. 2005;105(7):2724-2732.

23. Schaefer BC, Schaefer ML, Kappler JW, Marrack P, Kedl RM. Observation of antigen-dependent CD8+ T-cell/ dendritic cell interactions *in vivo*. *Cell Immunol*. 2001;214(2):110-122.

24. Mostbock S, Wu HH, Fenn T, et al. Distinct immune stimulatory effects of anti-human VISTA antibodies are determined by Fc-receptor interaction. *Front Immunol*. 2022;13:862757.

25. Masubuchi N, Araki M, Yang Y, et al. Mutant calreticulin interacts with MPL in the secretion pathway for activation on the cell surface. *Leukemia*. 2020;34(2):499-509.

26. Araki M, Yang Y, Imai M, et al. Homomultimerization of mutant calreticulin is a prerequisite for MPL binding and activation. *Leukemia*. 2019;33(1):122-131.

27. El-Khoury M, Cabagnols X, Mosca M, et al. Different impact of calreticulin mutations on human hematopoiesis in myeloproliferative neoplasms. *Oncogene*. 2020;39(31):5323-5337.

28. Gigoux M, Holmstrom MO, Zappasodi R, et al. Calreticulin mutant myeloproliferative neoplasms induce MHC-I skewing, which can be overcome by an optimized peptide cancer vaccine. *Sci Transl Med*. 2022;14(649):eaba4380.

29. Handlos Grauslund J, Holmstrom MO, Jorgensen NG, et al. Therapeutic cancer vaccination with a peptide derived from the calreticulin exon 9 mutations induces strong cellular immune responses in patients with CALR-mutant chronic myeloproliferative neoplasms. *Front Oncol*. 2021;11:637420.

30. Stein H, Bob R, Dürkop H, et al. A new monoclonal antibody (CAL2) detects CALRETICULIN mutations in formalin-fixed and paraffin-embedded bone marrow biopsies. *Leukemia*. 2016;30(1):131-135.

31. Kihara Y, Araki M, Imai M, et al. Therapeutic potential of an antibody targeting the cleaved form of mutant calreticulin in myeloproliferative neoplasms. *Blood*. 2020;136(suppl 1):9-10.

32. Achyutuni S, Nivarthi H, Majoros A, et al. Hematopoietic expression of a chimeric murine-human CALR oncoprotein allows the assessment of anti-CALR antibody immunotherapies in vivo. *Am J Hematol*. 2021;96(6):698-707.

33. Tvorogov D, Thompson-Peach CAL, Fosselteder J, et al. Targeting human CALR-mutated MPN progenitors with a neoepitope-directed monoclonal antibody. *EMBO Rep*. 2022;23(4):e52904.

34. Wang X, Mathieu M, Brezski RJ. IgG Fc engineering to modulate antibody effector functions. *Protein Cell*. 2018;9(1):63-73.

35. Uetrecht J. Immune-mediated adverse drug reactions. *Chem Res Toxicol*. 2009;22(1):24-34.

36. Temming AR, de Taeye SW, de Graaf EL, et al. Functional attributes of antibodies, effector cells, and target cells affecting NK cell-mediated antibody-dependent cellular cytotoxicity. *J Immunol*. 2019;203(12):3126-3135.

37. Prichard KL, O'Brien NS, Murcia SR, Baker JR, McCluskey A. Role of clathrin and dynamin in clathrin mediated endocytosis/synaptic vesicle recycling and implications in neurological diseases. *Front Cell Neurosci*. 2022;15:754110.

38. Li J, Xia Y, Kuter DJ. Interaction of thrombopoietin with the platelet c-mpl receptor in plasma: binding, internalization, stability and pharmacokinetics. *Br J Haematol*. 1999;106(2):345-356.

39. Cleyrat C, Darehshouri A, Steinkamp MP, et al. Mpl traffics to the cell surface through conventional and unconventional routes. *Traffic*. 2014;15(9):961-982.

40. Ibarra J, Elbanna YA, Kurylowicz K, et al. Type I but not type II calreticulin mutations activate the IRE1α/XBP1 pathway of the unfolded protein response to drive myeloproliferative neoplasms. *Blood Cancer Discov*. 2022;3(4):298-315.

41. Cabagnols X, Defour JP, Ugo V, et al. Differential association of calreticulin type 1 and type 2 mutations with myelofibrosis and essential thrombocytemia: relevance for disease evolution. *Leukemia*. 2015;29(1):249-252.

42. Grinfeld J, Nangalia J, Baxter EJ, et al. Classification and personalized prognosis in myeloproliferative neoplasms. *N Engl J Med*. 2018;379(15):1416-1430.

43. Tefferi A. Primary myelofibrosis: 2023 update on diagnosis, risk-stratification, and management. *Am J Hematol*. 2023;98(5):801-821.

44. Tefferi A, Guglielmelli P, Larson DR, et al. Long-term survival and blast transformation in molecularly annotated essential thrombocythemia, polycythemia vera, and myelofibrosis. *Blood*. 2014;124(16):2507-2615.

45. Knudsen TA, Skov V, Stevenson K, et al. Genomic profiling of a randomized trial of interferon-alpha vs hydroxyurea in MPN reveals mutation-specific responses. *Blood Adv*. 2022;6(7):2107-2119.

46. Mosca M, Hermange G, Tisserand A, et al. Inferring the dynamics of mutated hematopoietic stem and progenitor cells induced by IFNα in myeloproliferative neoplasms. *Blood*. 2021;138(22):2231-2243.

47. Prins D, Park HJ, Watcham S, et al. The stem/progenitor landscape is reshaped in a mouse model of essential thrombocythemia and causes excess megakaryocyte production. *Sci Adv*. 2020;6(48):eabd3139.

48. Ivanov D, Milosevic Feenstra JD, Sadovnik I, et al. Phenotypic characterization of disease-initiating stem cells in *JAK2*- or *CALR*-mutated myeloproliferative neoplasms. *Am J Hematol*. 2023;98(5):770-783.